Conditions and Mechanisms of Gas Emissions from Didymium Electrolysis and Its Process Control

Ksenija Milicevic, Dominic Feldhaus, and Bernd Friedrich

Abstract

During molten salt electrolysis of rare earths greenhouse gas emission occurs causing environmental and climate changes. In this study the electrochemical process window for didymium oxy-fluoride electrolysis is determined by linear sweep voltammetry and staircase chronoamperometry. Simultaneously the composition and the quantity of gas generation are investigated by an in situ FTIR-spectrometry in order to understand the process phenomena happening at anode and the mechanisms behind them. Different electrolyte compositions based on NdF_3, PrF_3 and LiF and various oxide amounts were employed showing the diversity in off-gas ratios. Effects of using two praseodymium-oxide compounds, namely Pr_6O_{11} and Pr_2O_3 used as raw materials, on the process and amount of anodic gases is considered as well. Perfluorocarbon (PFC) emission reduction is accomplished by electrolysis automatization by coupling the FTIR-spectrometer with a controller which triggers the oxide dosage preventing full anode effect.

Keywords

Didymium • PFC emission • Electrolysis
Greenhouse gas

Introduction

Current increase in price for neodymium (Nd) and praseodymium (Pr) oxide by +50% is direct consequence of their application boost in green technologies, such as wind turbines and electric cars, where didymium alloy (a mixture of Nd and Pr) is one of the main components of permanent magnets. This demand expansion leads to bigger neodymium and praseodymium production and therefore a rise of greenhouse gases (PFCs, CO_2) emission. Didymium alloy is usually produced by melting the defined mixture of pure neodymium and praseodymium metals which are obtained by oxy-fluoride molten salt electrolysis similar to aluminium electrolysis. Since separation of neodymium and praseodymium by solvent extraction is difficult and costly process due to their similar physical properties and knowing that praseodymium even improves some magnetic properties of Nd-based magnets [1–3] employing direct molten salt electrolysis of their mixed oxides is more advantageous. Another advantage is that the mixed Nd/Pr-oxide supplied as final product from magnet recycling, can be used for direct didymium production [4, 5] in place of primary extraction route during which the radioactive waste is present.

Nevertheless, due to the Chinese monopoly in rare earth metal production, scientists are confronted with the lack of and difficultly accessing scientific articles regarding didymium production by molten salt electrolysis. Some known papers [6, 7] in English report only the viability of the process but are without further explanations and are outdated, whereas accessible Chinese articles do not offer enough data [8–10]. Investigation on the influence of electrolyte composition on molten salt electrolysis of didymium was recently done [11] but information on off-gas emission is so far not known, initiating the research in this paper. Off-gas emission during neodymium electrolysis is already known [12–15] and is used as premise for didymium off-gas analysis.

Experimental

In all experiments a mixture of rare earth fluoride and lithium fluoride is used with 7:1 ratio at working temperature of approximately 1050 °C. The rare earth fluoride composition is varied as shown in Table 1. The chemicals used as electrolyte NdF_3 (Treibacher, $\geq$ 99.9%), PrF_3 (Treibacher, 99.9%) and LiF (Less common metals, >99.9%) were firstly

K. Milicevic (✉) · D. Feldhaus · B. Friedrich
IME Process Metallurgy and Metal Recycling, RWTH Aachen University, Aachen, Germany
e-mail: kmilicevic@ime-aachen.de

O. Martin (ed.), *Light Metals 2018*, The Minerals, Metals & Materials Series,
https://doi.org/10.1007/978-3-319-72284-9_187

Table 1 Electrolyte compositions

NdF_3 [wt%]	PrF_3 [wt%]	LiF [wt%]
87.5	0	12.5
78.75	8.75	12.5
64.23	23.27	12.5
57.75	29.75	12.5

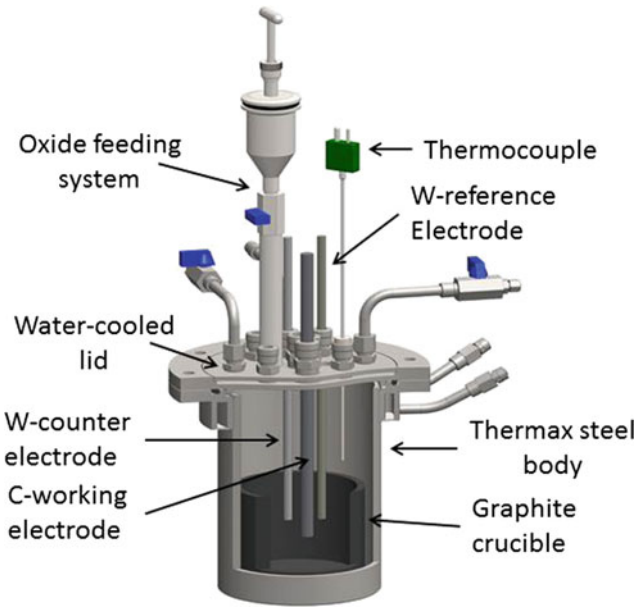

Fig. 1 Electrolysis cell setup

dried separately for 24 h at 250 °C, before they were accordingly mixed, pre-melted and homogenized in a high purity graphite crucible placed in a vacuum induction furnace under argon inert atmosphere at ca. 1050 °C. Such prepared electrolyte was stored under high purity argon atmosphere (O_2, H_2O <1 ppm) within a glovebox (Jacomex). Raw materials used Nd_2O_3 (Alfa Aesar, ≥99.9%), Pr_6O_{11} (Treibacher, ≥99.0%) and Pr_2O_3 (Treibacher, 99.61%) were dried for 24 h at 120 °C, pressed, crushed in pestle with mortar and sieved to particle size between 0.71 and 1.25 mm. The ratio of the dosed Nd/Pr-oxides was in all experiments 73.4–26.6 wt% and the concentrations used in electrolytes were varied between 0–4 wt%. The experimental setup consisted of pure graphite crucible (SIGRAFINE® R8510) filled with electrolyte (approx. 2 kg) and placed into steel closed cell with Swagelok connections through which the thermocouple type S with molybdenum sheath (Omega Engineering GmbH) and electrodes were inserted (Fig. 1). The lid of the cell is water cooled and had the dosing device for oxides built in. As working electrode (WE) high purity graphite rod (Ø6 mm, SIGRAFINE® R8510) was used, whereas tungsten rod served as quasi-reference (W-QRE) and counter (CE) electrode (Ø6 mm and Ø8 mm, respectively, with purity 99.95%). The prepared steel cell was placed in a resistance heated furnace and flushed with argon during whole experiments. All electrochemical measurements were carried out with an *IviumStat* potentiostat/galvanostat (Ivium Technologies B.V.). Simultaneously off-gas measurements were done by *Gasmet DX4000* Fourier transformation infrared spectrometer (FTIR, Ansyco). For the process control an appropriate software is installed in *Yokogawa UT55A* Controller for dosing the oxides if a certain voltage value is surpassed and/or CF_4 and C_2F_6 (PFC) gases were detected.

Results and Discussion

Process Window/off-Gas Composition

Linear sweep voltammograms of NdF_3–LiF (87.5–12.5 wt %) and NdF_3–PrF_3–LiF (64.23–23.27–12.5 wt%) electrolytes with different Nd_2O_3 and Nd_2O_3–Pr_6O_{11} (73.4–26.6 wt%) concentrations were recorded on graphite electrode with 5 mV/s scan rate which are shown in Fig. 2. Determined process window and off-gas composition for neodymium electrolysis (Fig. 2a) is used for comparison with phenomena happening during didymium electrolysis (Fig. 2b). Even now any firm conclusion on the mechanism of the anode process in aluminium electrolysis can't be given, which is used as basis for rare earth electrolysis. It is proposed that at low current densities the discharge of oxygen ions takes place at the most active sites on the anode surface, followed by its penetration into the carbon lattice and by further increase of current density in depletion at the anode surface [16]. Our neodymium experiments are comparable with previous research [12, 15] showing partial passivation with oxygen containing ions attributed to peak O_1 at around 1.7 V versus W-QRE where concentration of these electroactive species reaches its maximum resulting in high values of CO and CO_2 in off-gas. Anode current density depends on added oxide concentration and reaches a maximal value of 0.9 A/cm^2 with oxide concentration >2wt%. Afterwards full anode effect (O_2) happens at approx. 2.3 V versus W-QRE followed by current abrupt and PFC, namely CF_4 and C_2F_6 emission (Fig. 2a). In the case of electrolyte that contains PrF_3 and with addition of Pr_6O_{11} full anode effect is shifted more positive at around 3.0 V versus W-QRE due to the more complex component system

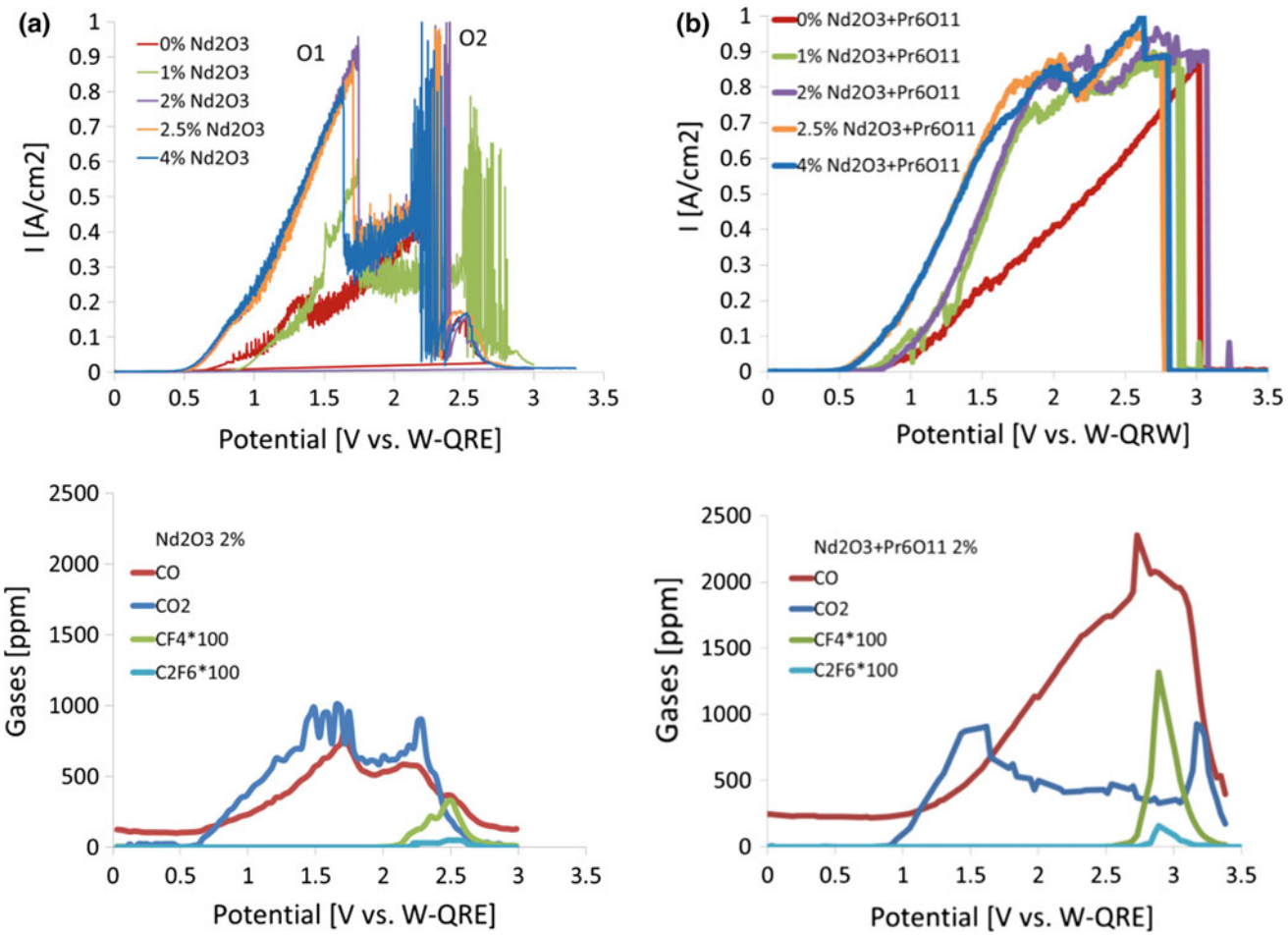

Fig. 2 **a** Linear sweep voltammograms recorded on graphite electrode at 1050 °C in NdF_3–LiF electrolyte with different Nd_2O_3 concentrations and scan rate = 5 mV/s (above) with off-gases measured with an in situ FTIR-spectrometer generated during electrochemical measurements with 2 wt% oxide (below); **b** Linear sweep voltammograms recorded on graphite electrode at 1050 °C in NdF_3–PrF_3–LiF electrolyte with different Nd_2O_3–Pr_6O_{11} concentrations and scan rate v = 5 mV/s (above) with off-gases measured with in situ FTIR-spectrometer generated during electrochemical measurements with 2 wt% oxide (below)

(Fig. 2b). Partial passivation occurs at the same current density values ca. 0.9 A/cm^2 but in this case without sharp current drop which is noticed in neodymium electrolysis. This difference can be explained by various simultaneous reactions of neodymium and praseodymium complex species. Proposed anodic reaction for neodymium by Stefanidaki [17] follows Eq. (1):

$$3[NdOF_5]^{4-} - 6e^- = 3/2O_2(g) + 3Nd^{3+} + 15\ F^- \quad (1)$$

Based on that we can propose same complex of praseodymium present in melt which oxidation as well generates oxygen on anode according to Eq. (2):

$$3[PrOF_5]^{4-} - 6e^- = 3/2O_2(g) + 3Pr^{3+} + 15\ F^- \quad (2)$$

Since the used Pr_6O_{11} consists of mixture of Pr^{4+} and Pr^{3+} some other complexes $[PrOF_x]^{y-}$ are probably present. The influence of praseodymium valence in oxide raw material on process and PFC emission is investigated in Sect. "Influence of Praseodymium Fluoride and Oxide on PFC Emission".

The composition of the off-gases during didymium electrochemical measurements is the same as in case of neodymium consisting of CO, CO_2, CF_4 and C_2F_6 as can be seen in Fig. 2a, b (showing one exemplar measurement with 2 wt% oxide for simplicity). Nevertheless, the ratio and amount differs and more gas is produced, especially CO/CO_2 ratio increases. C_2F_6 emission starts after CF_4 evolution showing the same tendency but with significantly smaller amount then during neodymium electrolysis. This increase in gas production is related to praseodymium molarity in its oxide and fluoride, i.e. higher oxygen and fluoride content and its availability. Additionally, Pr^{4+}-oxide present in Pr_6O_{11} reacts spontaneously with carbon ($\Delta G < 0$) following the Eq. (3) and evolution of CO and CO_2.

$$6PrO_2 + 2C = 3Pr_2O_3 + CO + CO_2 \quad (3)$$

Influence of Praseodymium Fluoride and Oxide on PFC Emission

In aluminium industrial electrolysis anode effect can occur up to several times per cell per day producing around 37.4 million metric tons of greenhouse gases worldwide [18]. This frequency of anode effect can be assumed for rare earth electrolysis requiring the analysis in which system and under which conditions the PFC has the highest emission. In Fig. 3 can be seen the tendency of anode effect and accordingly CF_4 evolution with increasing praseodymium content in NdF_3–PrF_3–LiF electrolyte and different Nd_2O_3–Pr_6O_{11} oxide concentration. In this figure the maximal CF_4 concentrations obtained during the measurements are taken into consideration after which electrolysis is interfered. It can be noticed that CF_4 amount decreases with increase of oxides in system and above 2 wt% remains relatively constant with increasing praseodymium content in electrolyte. This behavior is similar to aluminium electrolysis where wetting of the electrodes is worsened by alumina decrease leading to spread out of the gas bubbles and increase of their concentration on an anode [19] which in our case due to vertical position of used anode manages to escape the bath. There is so far no known research on the solubility of mixed didymium oxide in its fluoride salts but those results can implicate this chemical property as well. Nevertheless, the off-gas concentration values should be more considered for qualitative description of the systems and processes rather than for quantification of the off-gases due to many diverse influencing factors.

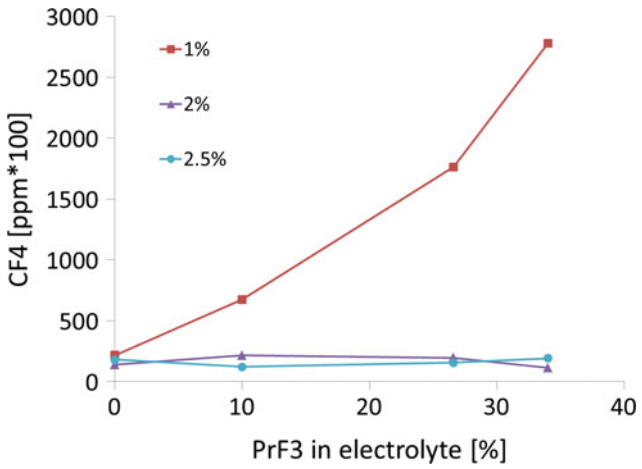

Fig. 3 Maximum CF_4 concentration in ppm * 100 in off-gas during electrochemical measurements in different NdF_3–PrF_3–LiF electrolyte systems with increasing praseodymium weight percentage and with different oxide amounts at 1050 °C measured by FTIR-spectrometer

Influence of Praseodymium Valence on Process Window and off-Gas Composition

The systems containing Pr_2O_3 with Pr^{3+} and Pr_6O_{11} with mixture of Pr^{3+} and Pr^{4+} are investigated and compared. Linear sweep voltammogram of NdF_3–PrF_3–LiF system with different concentrations of Nd_2O_3–Pr_2O_3 is shown in Fig. 4a expressing quite similar trend as the voltammograms done in the neodymium system without praseodymium (Fig. 2a). This behavior was expected, since in this case praseodymium and neodymium have the same valence 3^+ and close decomposition potentials of −1.276 V and −1.297 V, respectively calculated by FactSage® thermodynamical software at 1050 °C. The partial passivation with oxygen containing ions (peak O_1) is clear to distinguish from anode effect (peak O_2) and these reactions are happening at almost the same potentials, ca. 1.7 V versus W-QRE and ca. 2.3 V versus W-QRE, respectively. Higher current densities are notable owing it to simultaneous oxidation reactions of neodymium and praseodymium oxy-fluoride complexes shown in Eqs. (1) and (2) reaching the values of around 1.4 A/cm^2. The process window difference between systems using Pr^{3+} and mixture of Pr^{3+} and Pr^{4+} in same electrolyte presented in Fig. 4b clearly shows that additional oxidation reactions are taking part in systems containing Pr^{4+} ions. As assumed Pr^{4+} present in Pr_6O_{11} forms as well some other oxy-fluoride complexes which are shifting the critical potential values more positive and disable visibility of partial passivation by oxygen containing species.

Principle and Implementation of Process Control

Electrolysis process control is usually focused on cell potential and oxide concentration values. Since oxide concentration is quite difficult to measure in situ and online, critical cell potential data are used to build a controller with help of company *Yokogawa,* which would trigger the dosing of the oxides by reaching this pre-set potential value [20]. Chronoamperometry measurements are done on chosen potentials near oxidation reactions (O_1 and O_2) (Fig. 5a), allowing longer reaction time, during which off-gases are measured (Fig. 5b) in order to confirm our results and assumptions that CF_4 emission is detectable before full anode effect occurs. As it can be seen CF_4 evolution happens prior the full anode effect and after partial passivation, whereas C_2F_6 is detectable afterwards when an anode effect starts. From it can be concluded and confirmed that in partial passivation only oxygen containing species are taking part and CF_4 emission starts later at higher potentials. These findings led to possibility for installment of an advanced process control by connecting the FTIR-spectrometer (*Ansyco*) with new model controller *UT55A*. As soon as

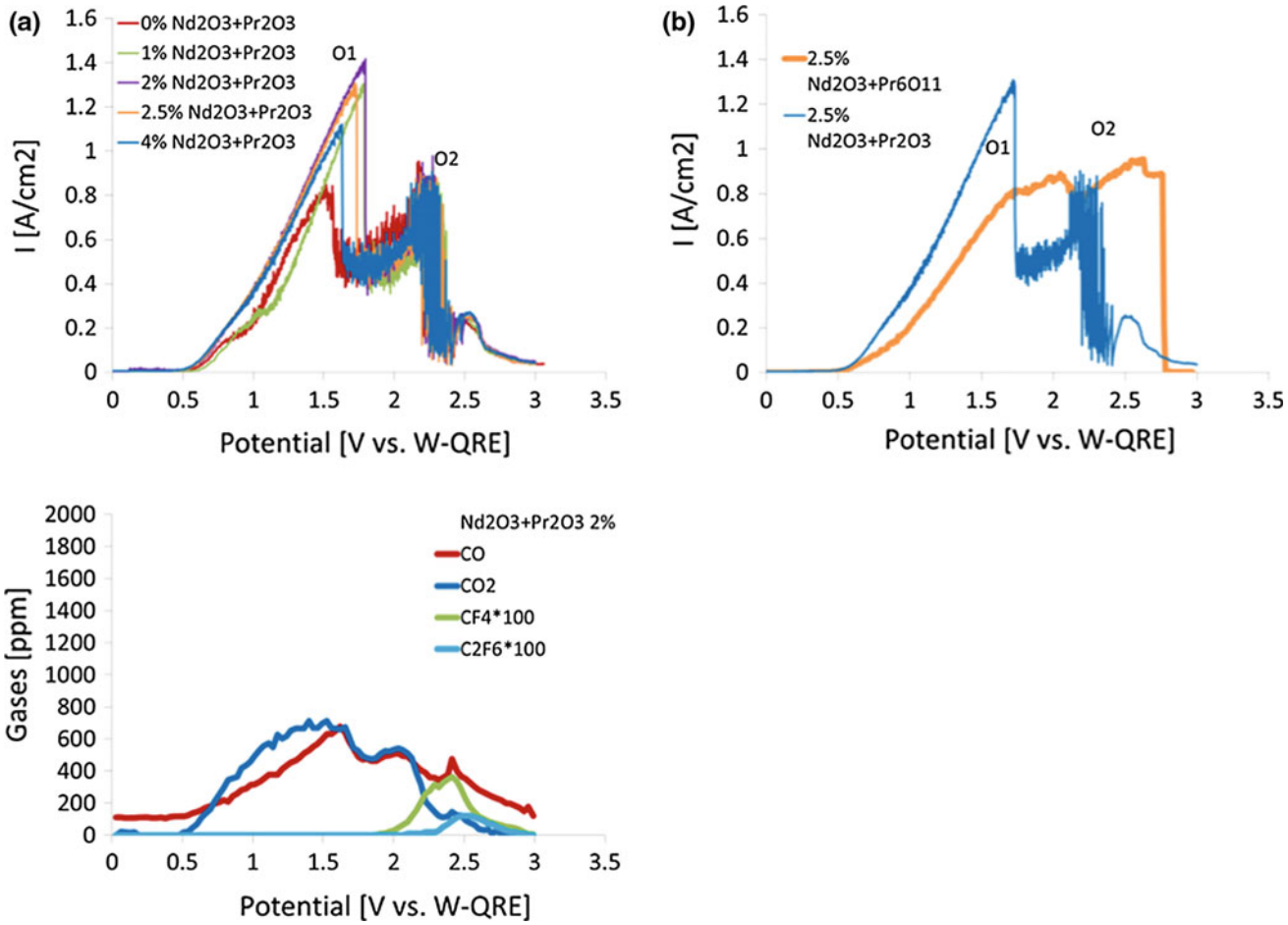

Fig. 4 **a** Linear sweep voltammograms recorded on graphite electrode at 1050 °C in NdF_3–PrF_3–LiF (64.23–23.27–12.5 wt%) electrolyte with different Nd_2O_3–Pr_2O_3 (73.4–26.6 wt%) concentrations and scan rate = 5 mV/s (above) with off-gases measured with an in situ FTIR-spectrometer generated during these measurements in case with 2 wt% oxide (below) b) Comparison of process windows in NdF_3–PrF_3–LiF electrolyte with 2.5 wt% Nd_2O_3–Pr_6O_{11} and Nd_2O_3–Pr_2O_3

previously-set PFC concentrations are detected by in situ FTIR-spectrometer, the signal will be send to controller, triggering again the dosing of the oxides and preventing full anode effect.

Conclusion and Outlook

Process windows for neodymium electrolysis (as reference) and didymium molten salt electrolysis in different electrolytes, using diverse mixed oxide concentrations and with two different praseodymium oxides, namely Pr_2O_3 and Pr_6O_{11}, were determined. Critical potential for full anode effect differs only in case when Pr_6O_{11} is used as the raw material leading to a more positive shift of anode potential values and impedes visibility of partial passivation by oxygen containing species. Presumably, next to present $[NdOF_5]^{4-}$ and assumed $[PrOF_5]^{4-}$ at least one more praseodymium oxy-fluoride complex exists taking part in oxidation reactions on the anode. Simultaneously, the off-gases were measured in situ by FTIR-spectrometer and analyzed. In regard to PFC emission the use of higher praseodymium fluoride content in electrolyte showed higher CF_4 and C_2F_6 concentrations in case of anode effect, when the oxide amount was below 2 wt %. Investigations show that CF_4 can be detected before full anode effect, whereas C_2F_6 is emitted at and after this phenomenon. This fact was used for installment of a controller triggering the oxide dosing after first CF_4 detection preventing the system entering full anode effect. Next step will be implementation of those fundamental findings into

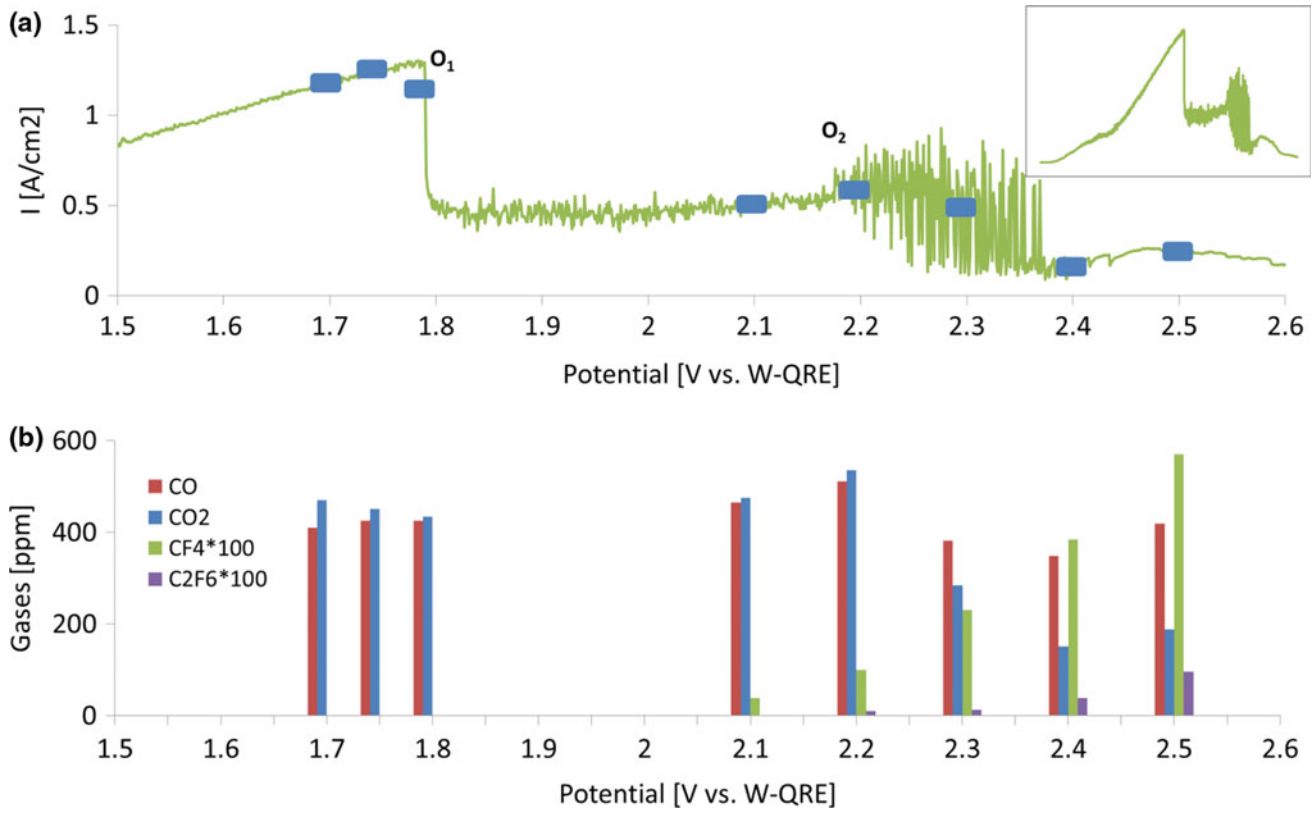

Fig. 5 **a** Chosen potentials for chronoamperometry presented on linear sweep voltammogram of NdF_3–PrF_3–LiF (64.23–23.27–12.5 wt%) system with 1 wt% Nd_2O_3–Pr_2O_3 (whole voltammogram in inset). **b** Off-gas composition during the chronoamperometry on potentials marked in figure (**a**)

scaled-up long-term electrolysis with similar setup to an industrial one in order to estimate the feasibility of the process control, i.e. PFC emission reduction.

Acknowledgements This work was supported by the FP-7 EU Program Grant No. 309373 "Development of a Sustainable Exploitation Scheme for Europe's rare earth Deposits" (EURARE).

References

1. Sun H et al. (2011) Coercivity enhancement in Nd–Fe–B sintered permanent magnet doped with Pr nanoparticles. Journal of Applied Physics 109 (7):07A749.
2. McGuiness PJ, Podmiljsak B, Kobe S (2003) The effect of Pr and Zr substitutions on the disproportionation reaction in Nd-Fe-B-based materials. IEEE Transactions on Magnetics 39 (5):2956–2958.
3. Kablov EN et al. (2005) Effect of Praseodymium on Magnetic Properties and Phase Composition of a Material of the Nd–Pr–Dy–Fe–Co–B System. Metal Science and Heat Treatment 47(5–6): 227–231.
4. Nakamoto M et al. (2012) Extraction of Rare Earth Elements as Oxides from a Neodymium Magnetic Sludge. Metallurgical and Materials Transactions B 43(3):468–476.
5. Kruse S et al. (2017) Influencing Factors on the Melting Characteristics of NdFeB-Based Production Wastes for the Recovery of Rare Earth Compounds. Journal of Sustainable Metallurgy 3(1):168–178.
6. Morrice E, Henrie TA (1967) Electrowinning high-purity neodymium, praseodymium, and didymium metals from their oxide. Report of investigations, United States Department of the Interior, Bureau of Mines, Washington D.C.
7. Tamamura H (1990) Process for preparing praseodynium metal or praseodymium-containing alloy US. Patent US4966662 A. 30 October 1990.
8. Liu Y et al. (2016) Effects of Physical Properties of Pr-Nd Oxide on its Electrolysis Preparation and Improvement Measures (in Chinese). Rare Metals and Cemented Carbides 44 (2):50–53.
9. Liu M, Wang L (2014) Study on the Effects of Electrolysis Temperature on Technical Indexes of Rare Earth Electrolytic Cell (in Chinese). Rare Metals and Cemented Carbides 42 (6):16–19.
10. Li J et al (2008) Carbon Content Control for Pr-Nd Alloy Production Process Using 6000 A Electrolysis Cell (in Chinese). Rare Metals Letters 27 (11):41–43.
11. Milicevic K, Meyer T, Friedrich B (2017) Influence of electrolyte composition on molten salt electrolysis of didymium. Presentation at The 2nd conference on European Rare Earth Resources, Santorini, Greece, 28–31 May 2017. https://doi.org/10.13140/RG.2.2.13137.33122.
12. Liu S et al. (2014) Anode processes for Nd electrowinning from LiF–NdF. Electrochimica Acta 147:82–86.
13. Vogel H et al. (2016) Reducing Greenhouse Gas Emission from the Neodymium Oxide Electrolysis. Part I: Analysis of the Anodic Gas Formation. Journal of Sustainable Metallurgy 3(1):99–107. https://doi.org/10.1007/s40831-016-0086-0.

14. Keller R, Larimer KT (1997) Anode effect in neodymium oxide electrolysis. In: Bautista, RG et al. (ed) Rare earths—science, technology and applications III. The Minerals, Metals and Materials Society, Warrendale, p 175–180.
15. Li B et al. (2014) Electrochemistry for Nd electrowinning from fluoride-oxide molten salts. In: Neale R et al. (ed) Rare Metal Technology. The Minerals, Metals & Materials Society, San Diego, p 95–98.
16. Grjotheim K et al. (1977) Aluminium electrolysis: The chemistry of the Hall-Héroult process. Aluminium-Verlag, Düsseldorf.
17. Stefanidaki E, Hasiotis C, Kontoyannis C (2001) Electrodeposition of neodymium from LiF–NdF_3–Nd_2O_3 melts. Electrochimica Acta 46 (17):2665–2670.
18. Chase R, Gibson R, Marks J (2005) PFC Emissions performance for the global primary aluminium industry. In: Kvande H (ed) Light metals 2005. The Minerals Metals & Materials Society, Warrendale, p 279–282.
19. Thonstad J, Utigard TA, Vogt H (2000) On the Anode Effect in Aluminum Electrolysis. In: Peterson RD (ed) Light Metals 2000. The Minerals Metals & Materials Society, Warrendale, p 249–256.
20. Vogel H, Friedrich B (2017) Reducing Greenhouse Gas Emission from the Neodymium Oxide Electrolysis. Part II: Basics of a Process Control Avoiding PFC Emission. International Journal of Nonferrous Metallurgy, 6 (3):27–46.